Electron-Magnon Scattering and Magnetization Switching in Perpendicularly Magnetized Thin Films and Nanowires

A. Mihai, C. Beigné, A. Marty, L. Vila, P. Warin, Y. Samson, J.P. Attané

Lab. Nanostructures et Magnétisme
CEA / Univ. Joseph Fourier
Grenoble, France

Reversal process of FePt/MgO thin layers

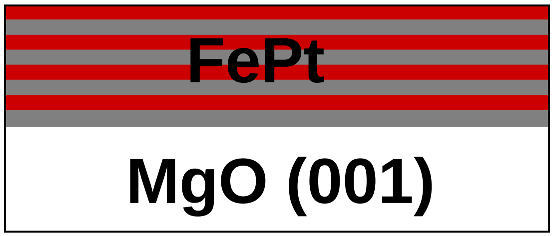

$B_A \sim 10T$

Thin layer with perpendicular magnetization

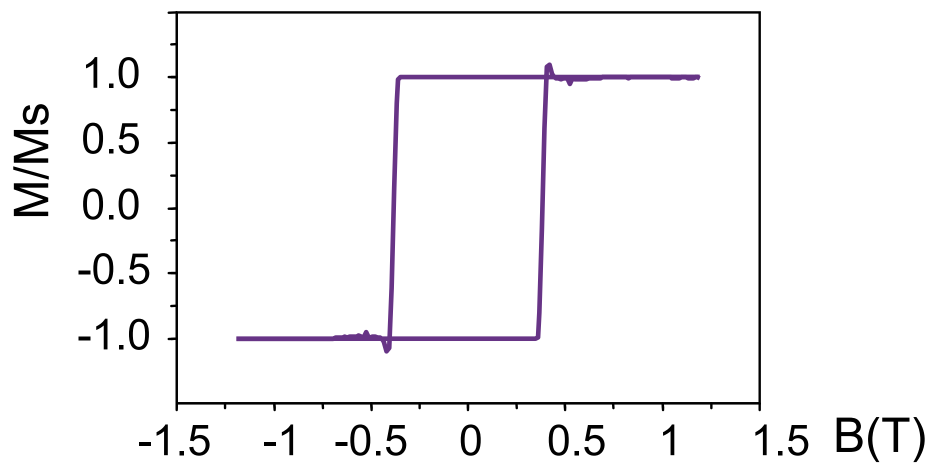

Hysteresis loop measured by E.H.E.

PRL **96**, (2006) 147204 ; PRL **93**, (2004) 257203

Resistivity measurements on FePt(10nm)

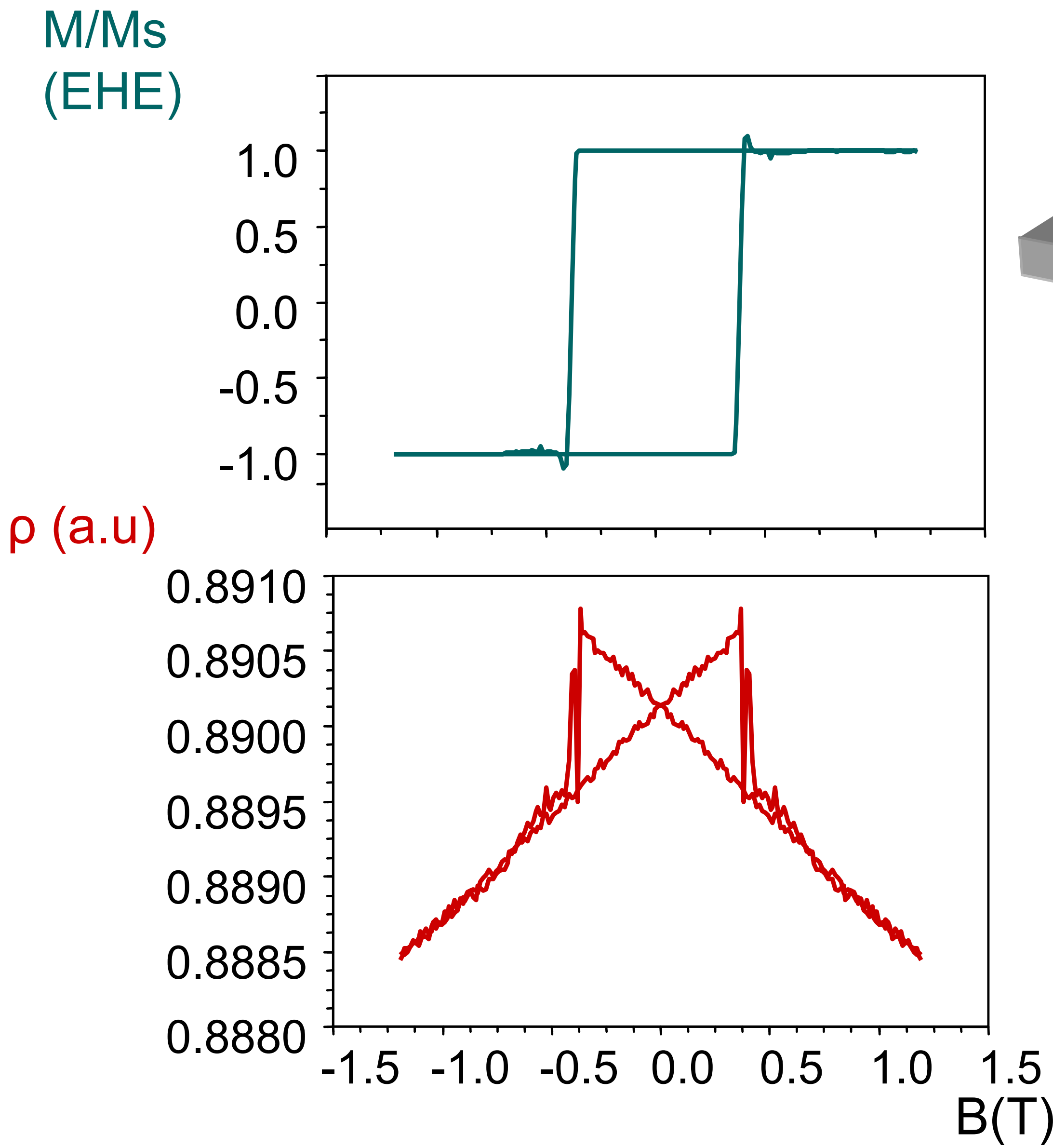

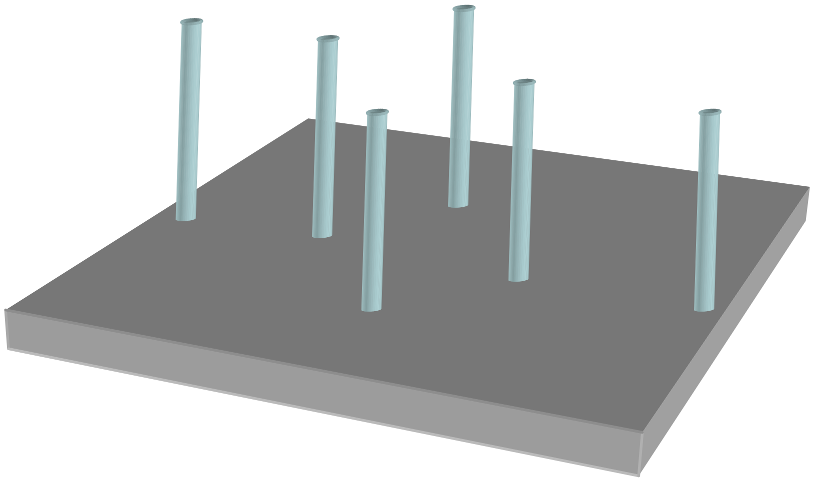

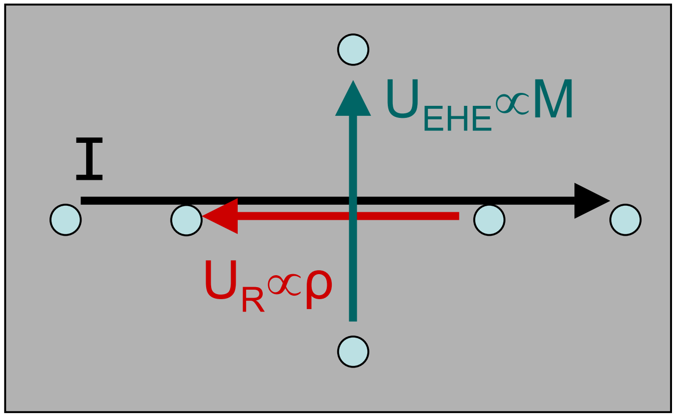

Resistivity contributions

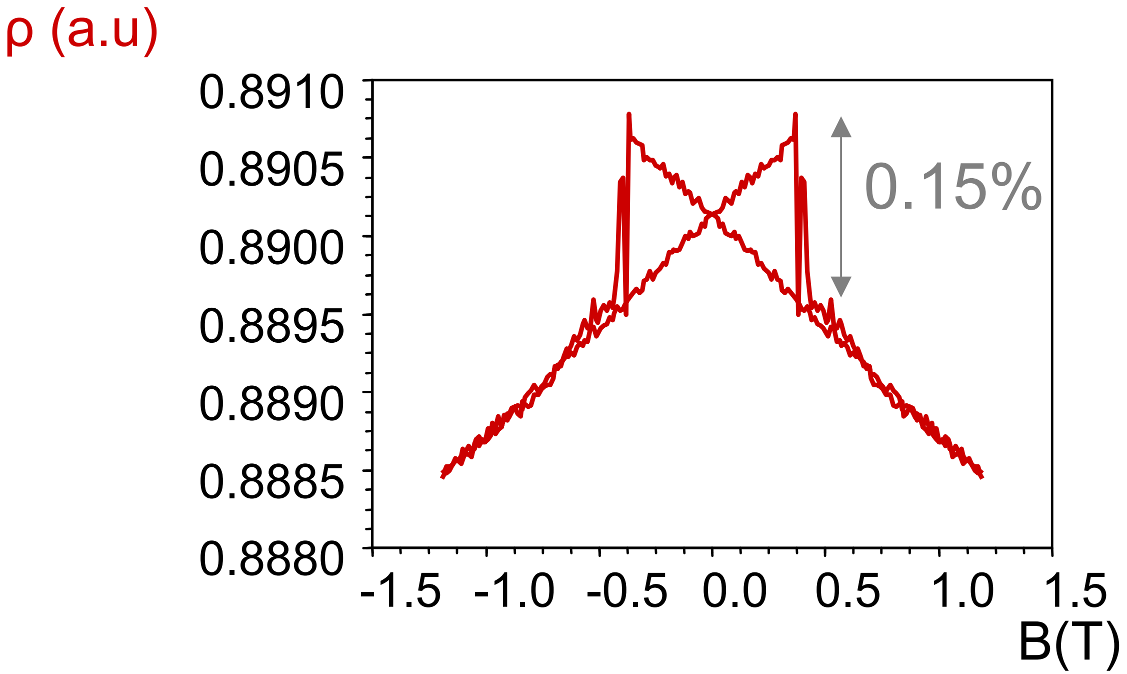

$$\rho = \rho_{imp} + \rho_{ph} + \rho_{e\text{-}e} + \rho_{he} + \rho_{ehe} + \rho_{dw} + \rho_{amr} + \ldots + \rho_{magn}$$

ρ_{MMR}

Resistivity measurements

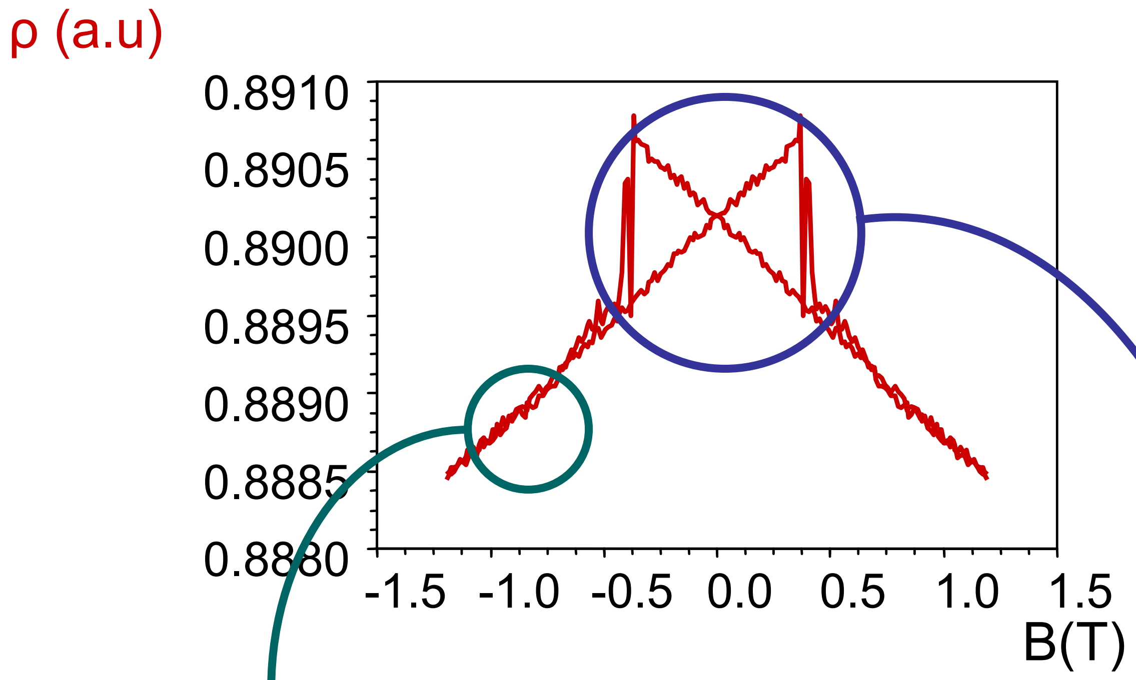

Saturated magnetization state :
$\rho_{MMR} \propto -|B|$

Magnetization reversal :
$\rho_{MMR} = f(B,M)$

Electron-magnon scattering and resistivity

PHYSICAL REVIEW B **66**, 024433 (2002)

Electron-magnon scattering and magnetic resistivity in 3*d* ferromagnets

B. Raquet,[1,*] M. Viret,[2] E. Sondergard,[2] O. Cespedes,[3] and R. Mamy[4]
[1]*Laboratoire National des Champs Magnétiques Pulsés (LNCMP), 143 Av. de Rangueil, 31432 Toulouse, France*
[2]*CEA, Saclay, Service de l'Etat Condensé, Orme des merisiers, 91191 Gif sur Yvette, France*
[3]*Physics Department, Trinity College, Dublin 2, Ireland*
[4]*Laboratoire de Physique de la Matière Condensée de Toulouse, 135 Av. de Rangueil, 31077 Toulouse, France*
(Received 26 November 2001; revised manuscript received 3 May 2002; published 25 July 2002)

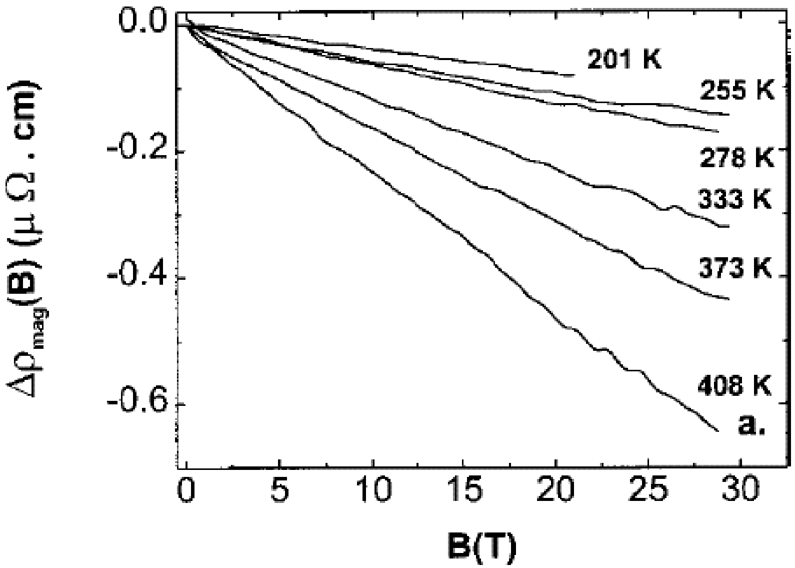

Fe(80 nm)/MgO

For high fields :
$\rho_{MMR} \propto -|B|$

Field dependance of the resistivity : $\rho \propto -|B|$

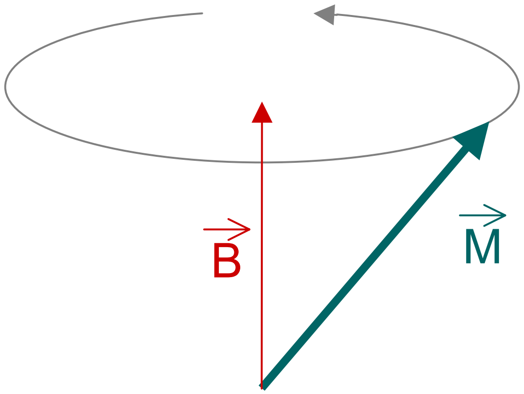

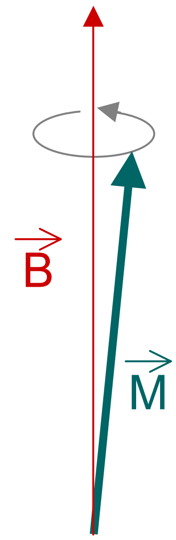

Weak applied field

High magnon population

High resistivity

Strong applied field

Low magnon population

Low resistivity

Raquet *et al.*'s model

Magnons dispersion relation :

$$E(k) \sim D\,k^2 + g\,\mu_B\,\underbrace{(B_{ext} + \mu_0\,M_S + B_A + B_D + \mu_0\,M_S\,\sin^2\theta_k\,)}_{B_E}$$

D exchange stiffness constant

g Landé factor

μ_B Bohr magneton

B_{ext} external field

B_A anisotropy field

B_D demagnetizing field

θ_k angle between k and M

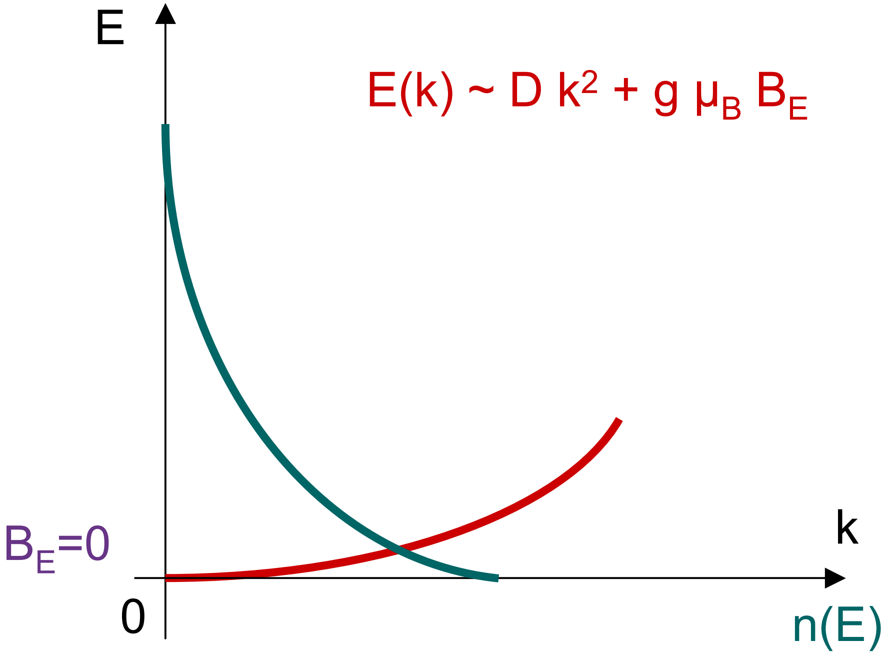

Raquet *et al.*'s model

Magnons dispersion relation :

$$E(k) \sim D\,k^2 + g\,\mu_B\,\underbrace{(B_{ext} + \mu_0 M_S + B_A + B_D + \mu_0 M_S \sin^2\theta_k)}_{B_E}$$

D exchange stiffness constant

g Landé factor

μ_B Bohr magneton

B_{ext} external field

B_A anisotropy field

B_D demagnetizing field

θ_k angle between k and M

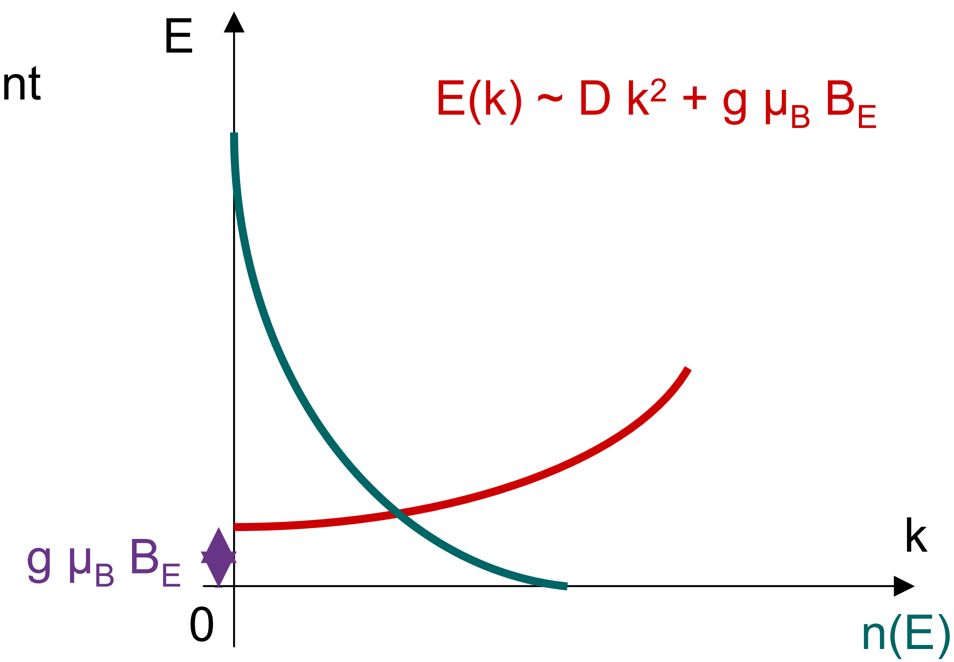

Raquet *et al.*'s model

Magnons dispersion relation :

$$E(k) \sim D\,k^2 + g\,\mu_B\,(\underbrace{B_{ext} + \mu_0 M_S + B_A + B_D + \mu_0 M_S \sin^2\theta_k}_{B_E})$$

D exchange stiffness constant

g Landé factor

μ_B Bohr magneton

B_{ext} external field

B_A anisotropy field

B_D demagnetizing field

θ_k angle between k and M

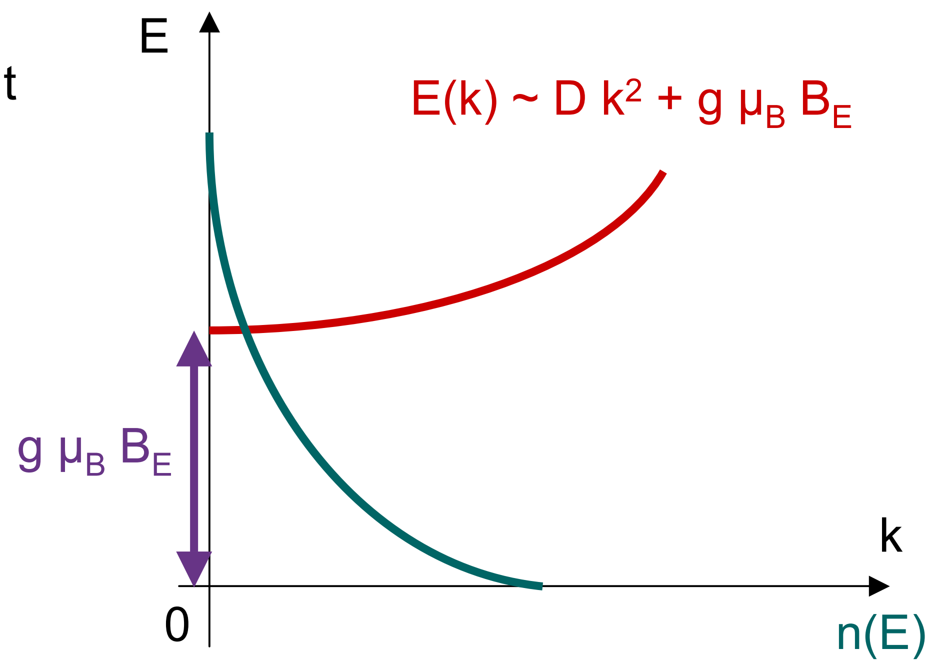

Raquet *et al.*'s model

Calculus of the electron-magnon interaction

$$E(k) \sim D\,k^2 + g\,\mu_B\,B_E \quad\longrightarrow\quad \rho_{MMR} \propto \frac{B_E}{D(T)^2}\,T\ln\left(\frac{g\mu_B B_E}{kT}\right)$$

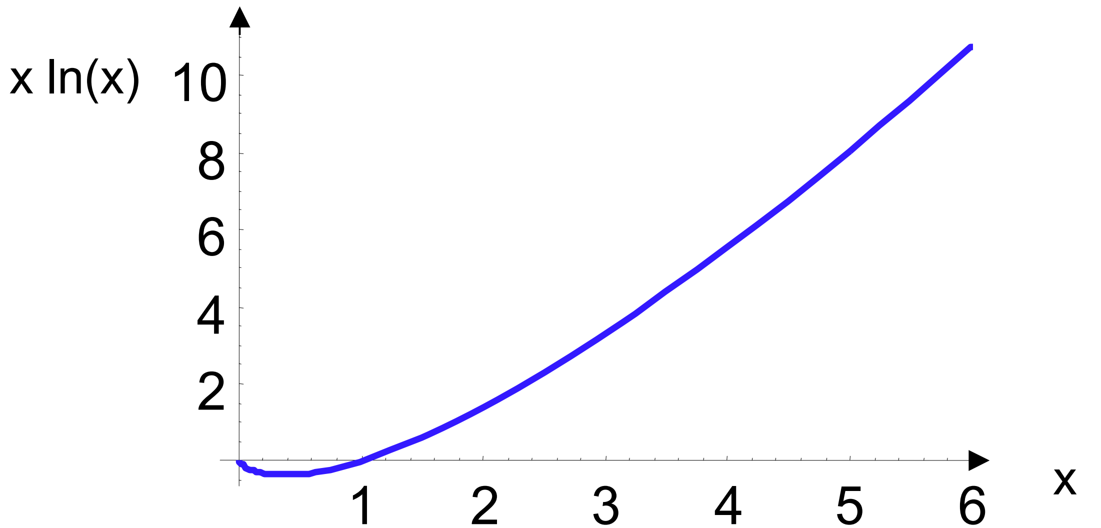

$\rho_{MMR} \propto B_E$ for large values of B_E

Linearity at the vicinity of zero field

Thin layers of 3d metals

$B_E \sim B_{ext}$

- no linearity near B_{ext}=0
- AMR contribution, etc.

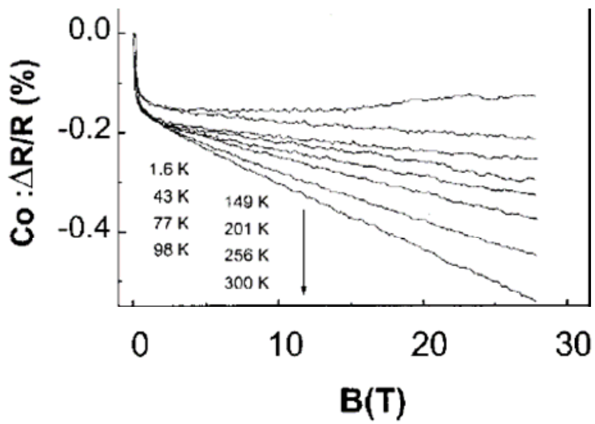

Thin FePt layers

$B_E \sim B_{ext} + B_A$

- linearity near B_{ext}=0
- remanent magnetic configuration

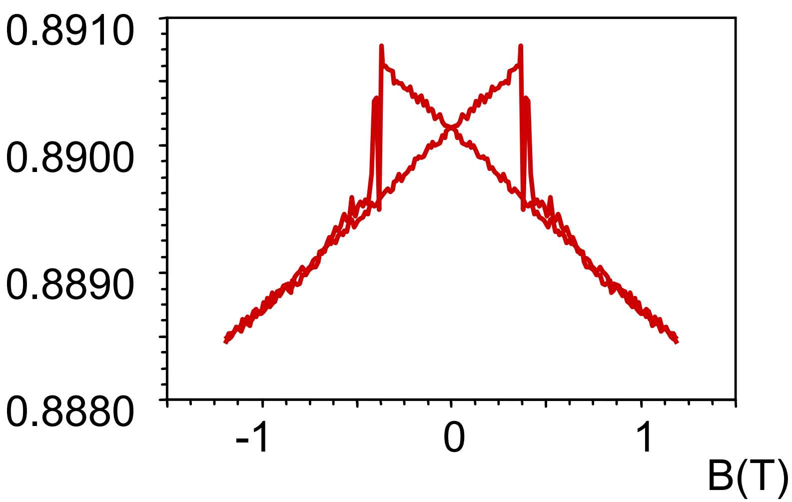

The sample being magnetically saturated,;

the equation

$\rho_{MMR} \propto B_{ext}$

Is still valid for B_{ext}<0

Temperature dependance

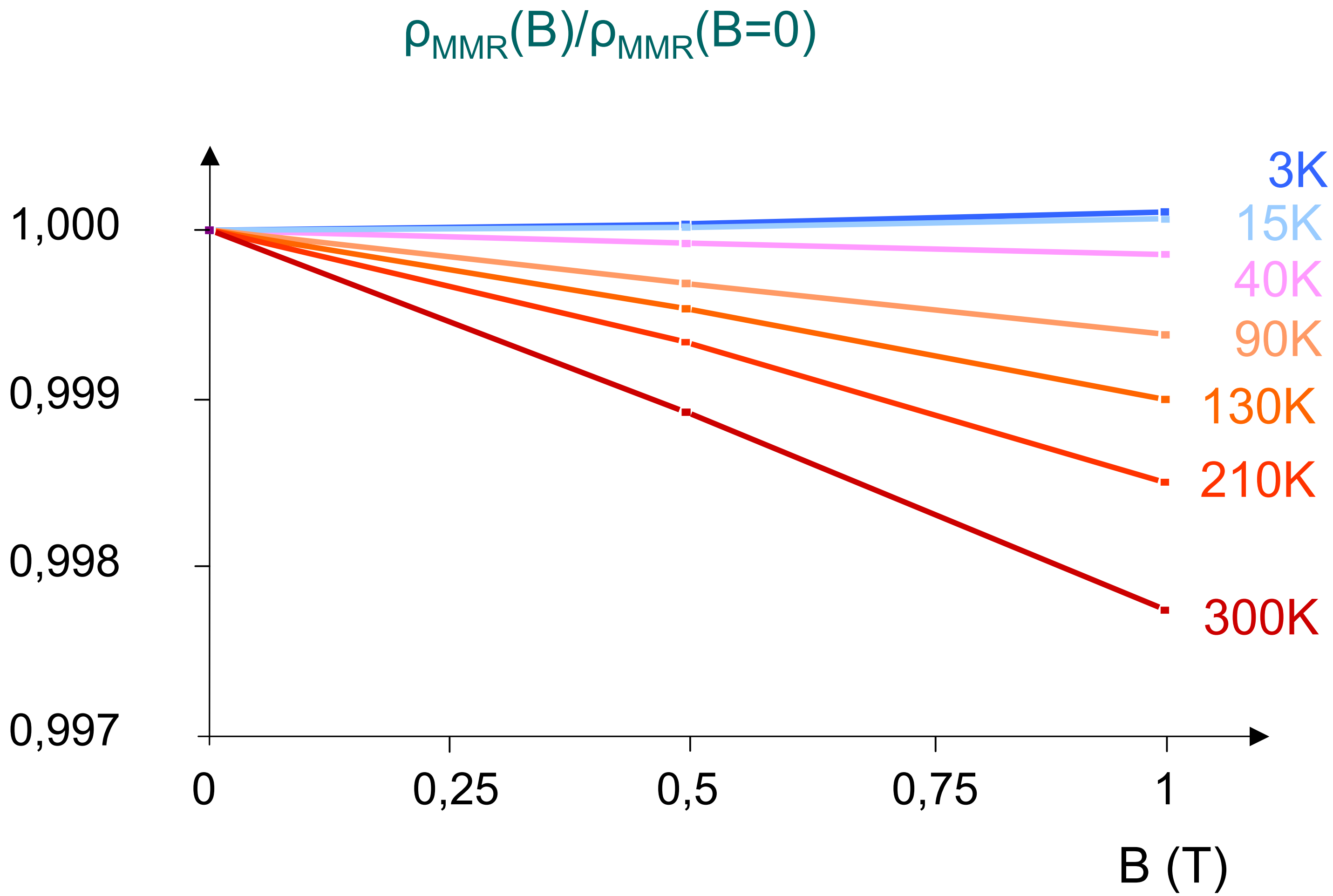

Magnetization reversal and MMR variations

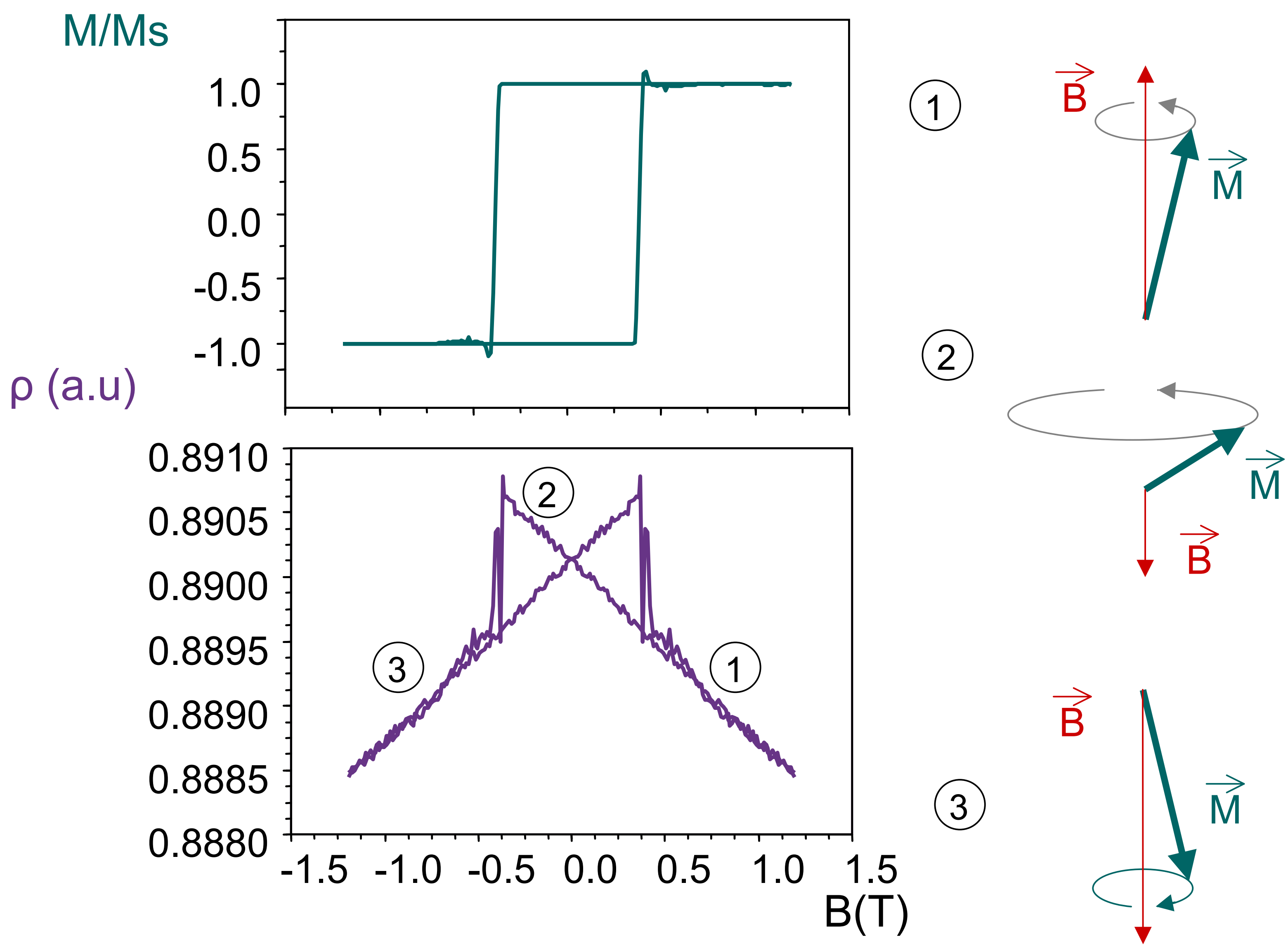

MMR and partially reversed states of magnetization

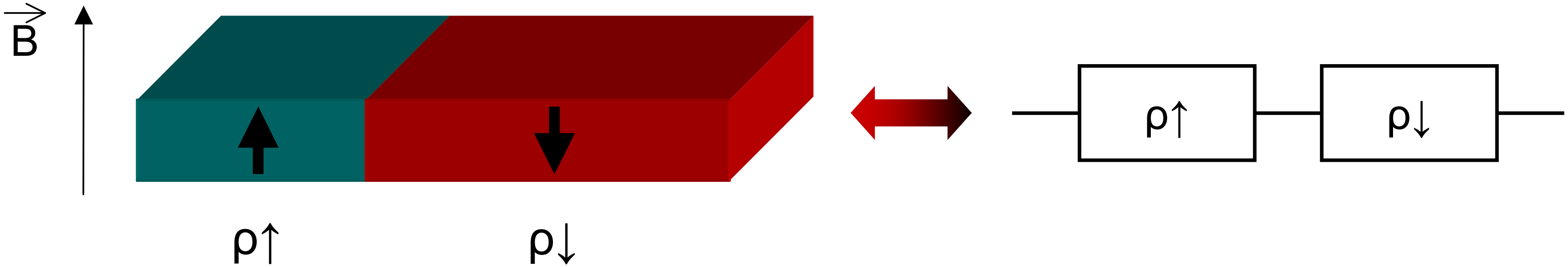

$V\uparrow = V_0(M/Ms + 1)/2$

$V\downarrow = V_0(1 - M/Ms)/2$

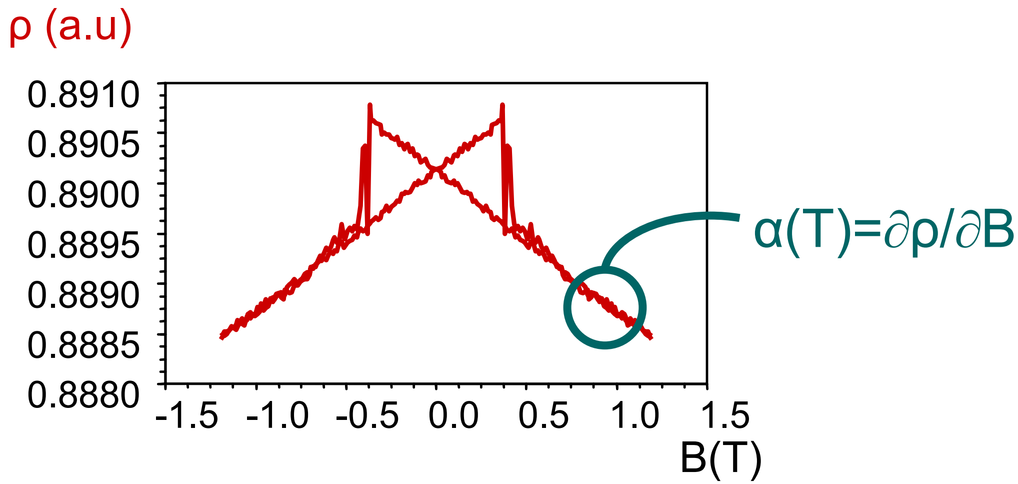

$$\rho_{MMR} = -\frac{M}{M_S}\alpha(T)B$$

Magnetization reversal detection using MMR measurements

$$\rho_{MMR} \propto M \times B$$

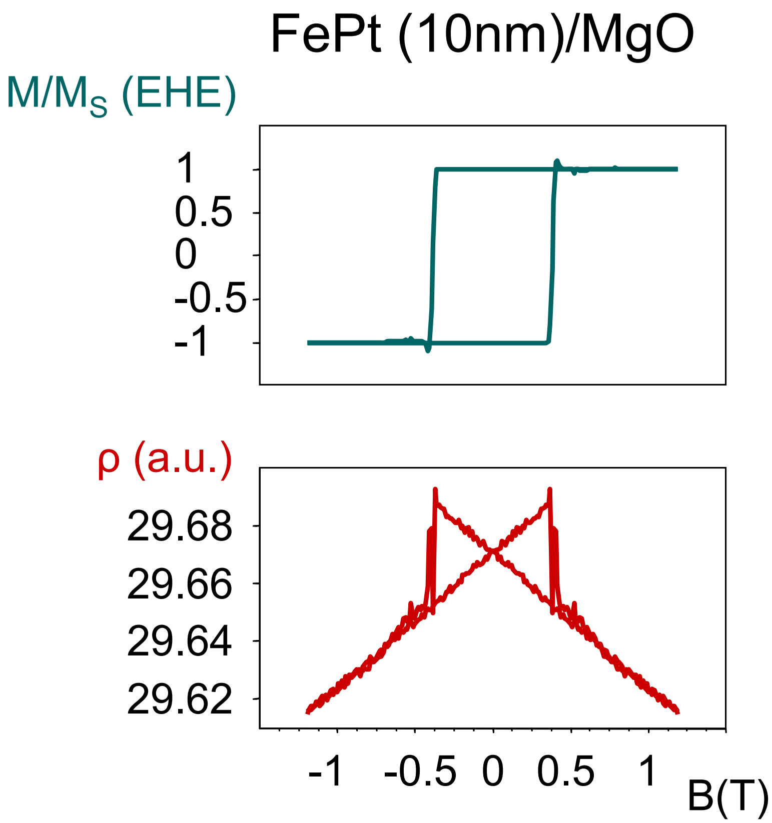

Magnetization reversal detection using MMR measurements

$$\rho_{MMR} \propto M \times B$$

FePt (10nm)/MgO

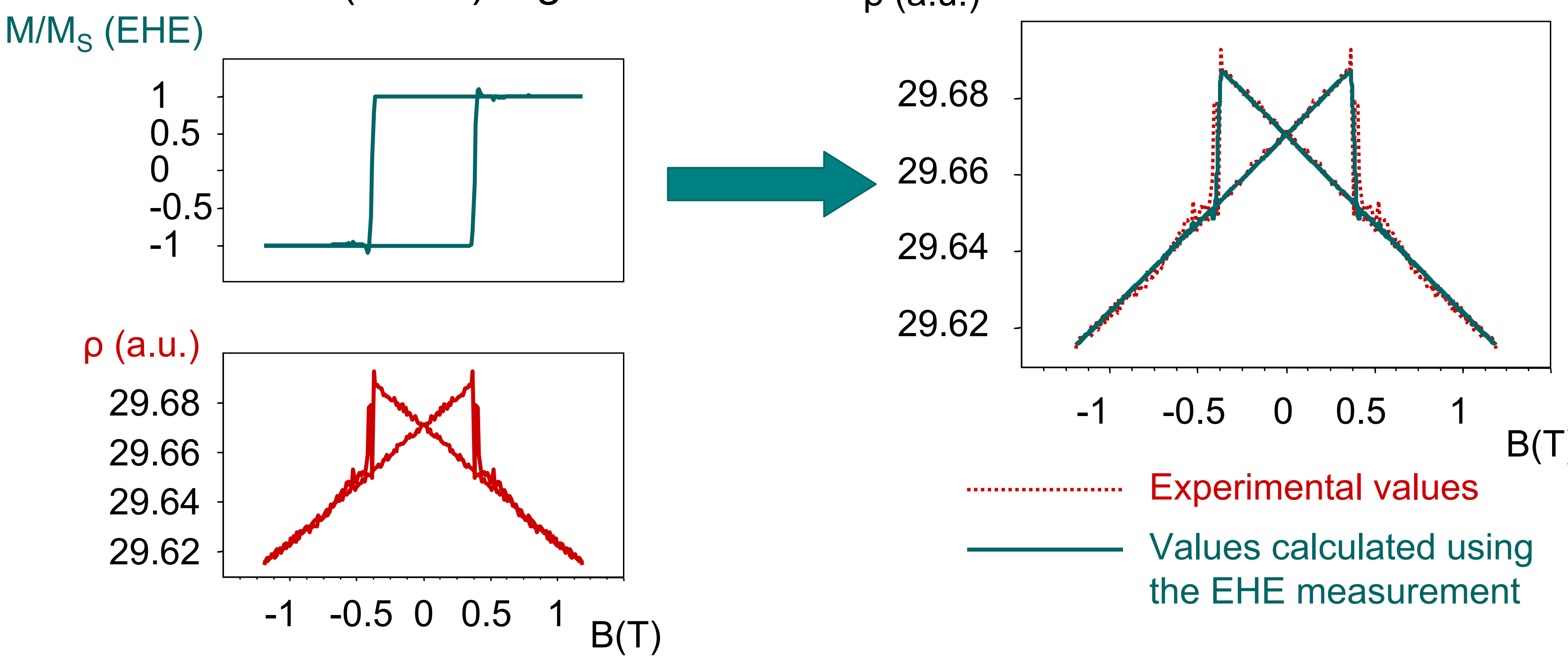

Magnetization reversal detection using MMR measurements

$\rho_{MMR} \propto M \times B$

FePt (32nm)/MgO

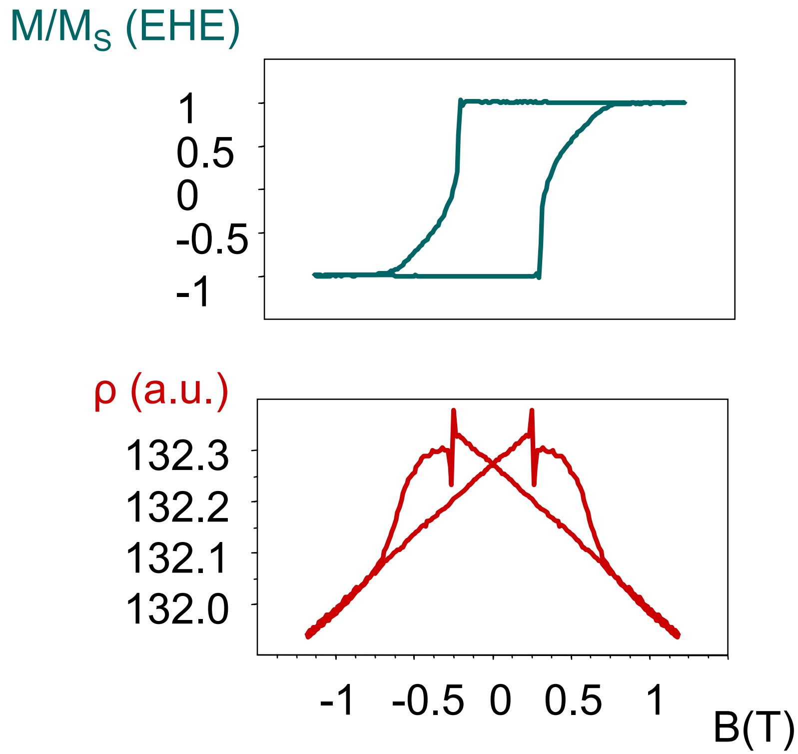

Magnetization reversal detection using MMR measurements

$$\rho_{MMR} \propto M \times B$$

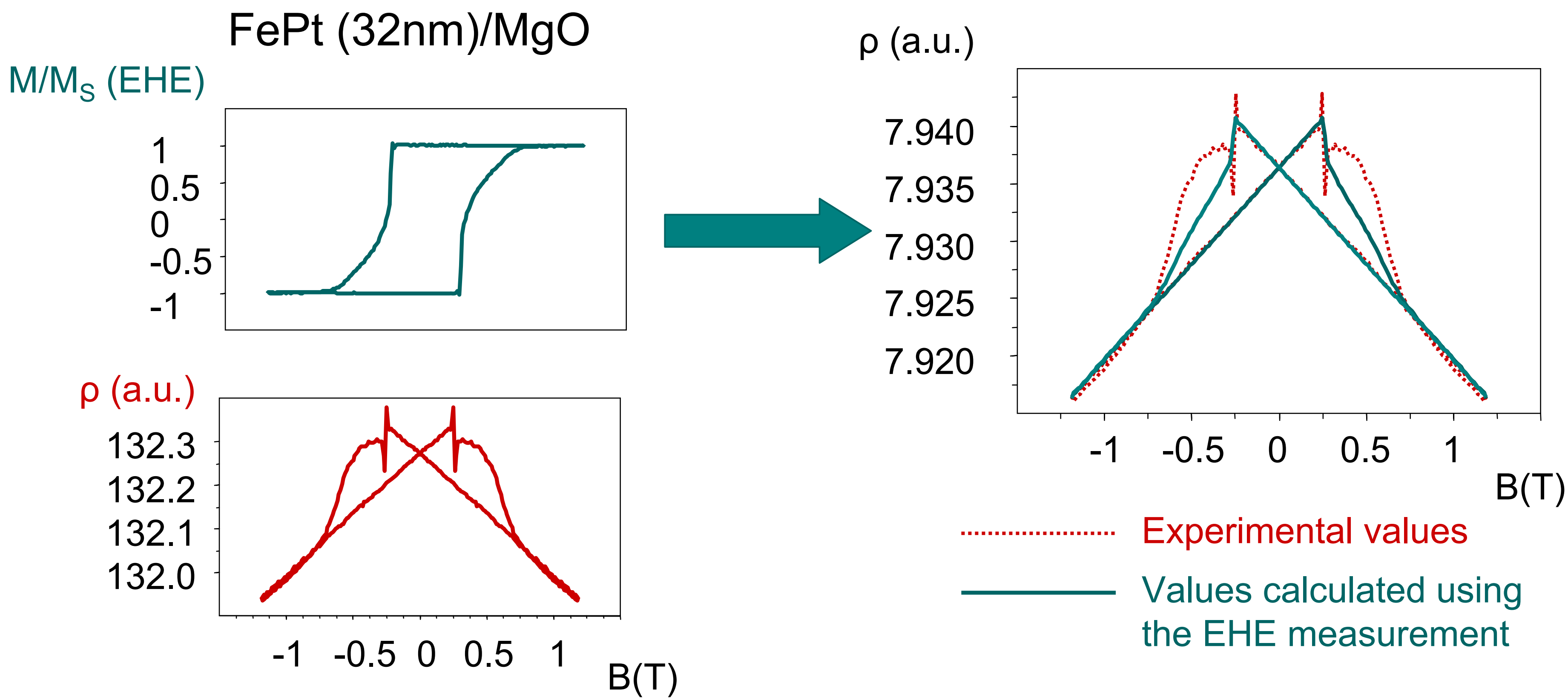

Localizing a Domain Wall within a Nanowire using MMR

$$\rho_{MMR} \propto M \times B$$

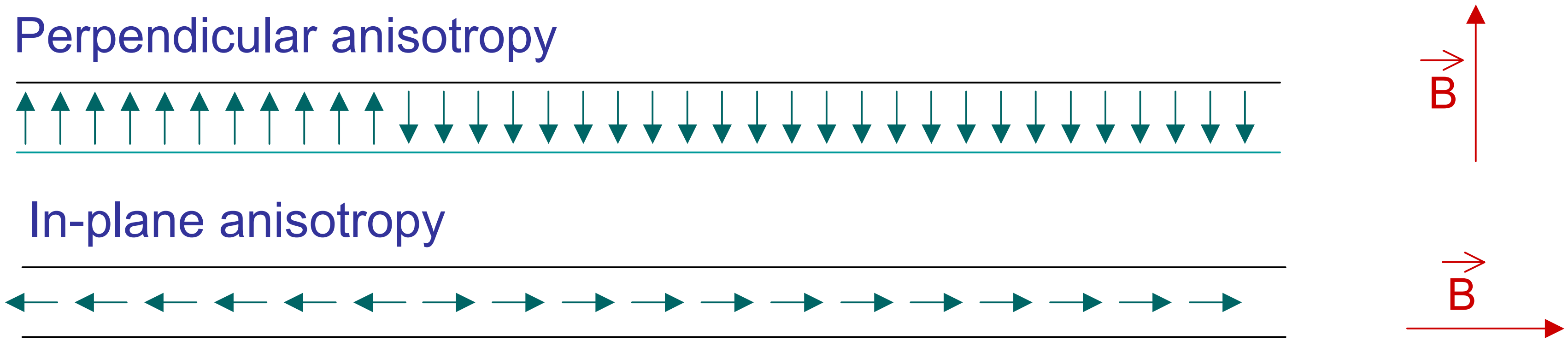

- Basically similar to GMR in CIP spin-valves, but with a single layer

- $\rho_{MMR} \propto M \times B \rightarrow$ necessity of applying a field

- limited to relatively highly anisotropic materials

Magnetization reversal detection within a nanowire

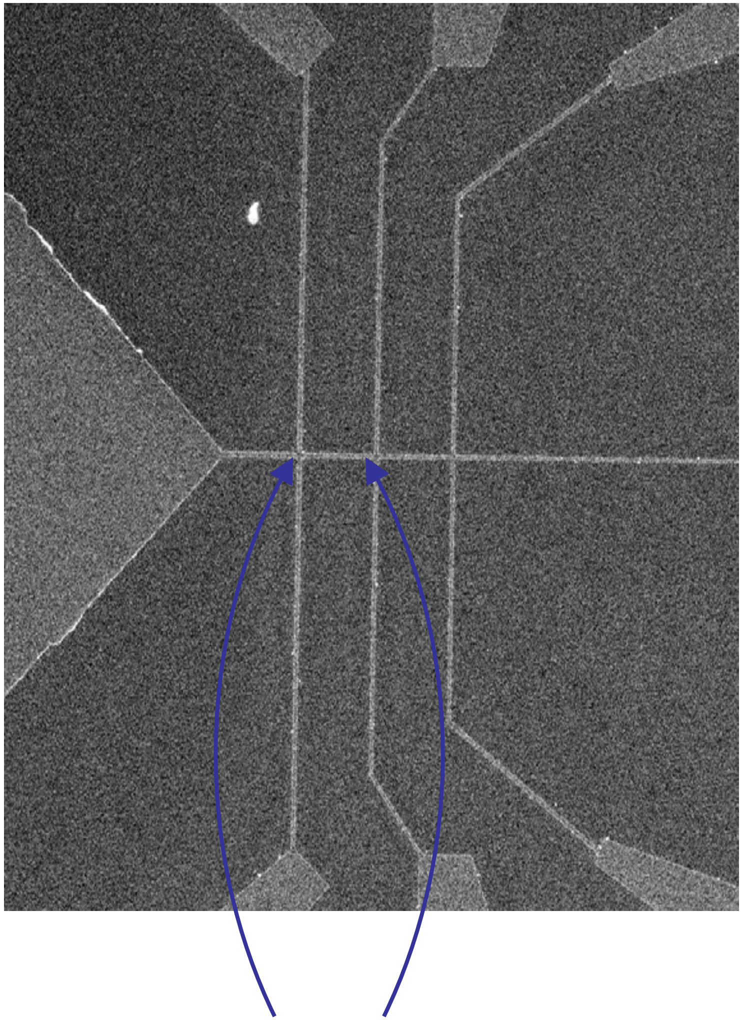

MEB observation of nanowires
150 nm×3 µm
FePt(10 nm)/MgO

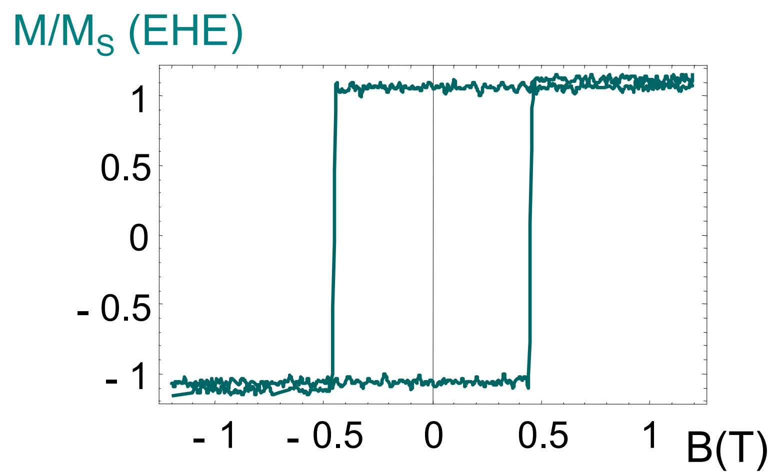

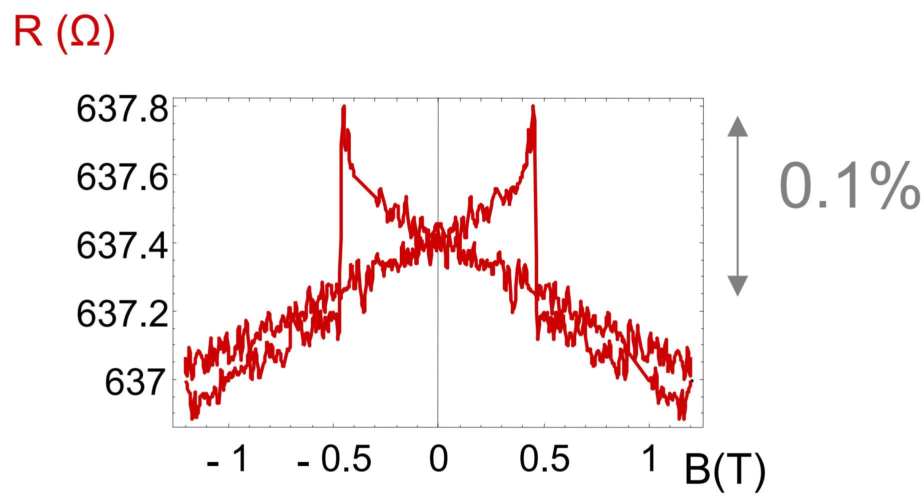

Conclusions

$$\rho_{MMR} \propto M \times B$$

- low signals, especially in materials with low H_C

$\rightarrow$ Measurement technique restricted to fundamental studies

- usable whenever two domains of opposite magnetization coexist

- necessity to get rid of DW resistance to measure M using MMR

- necessity to take MMR into account when measuring DW resistances

Mihai *et al.*,PRB **77**, 060401(R) (2008)

Temperature effects

$$\rho_{MMR} \propto \frac{B_t}{D(T)^2} T \ln\left(\frac{g\mu_B B_t}{kT}\right)$$

$$\begin{cases} D = D_0 - D_1 T^2 - D_2 T^{\frac{5}{2}} \\ B_t = B_0 + B \quad \text{avec} \quad B << B_0 = B_A + \mu_0 M_S \end{cases}$$

$$\Rightarrow \quad \frac{\partial \rho_{MRP}(T)}{\partial B} \propto \frac{T}{D(T)^2}\left[\ln(T) - \ln\left(\frac{\mu_B B_0}{k}\right) - 1 - \frac{B}{B_0} + \frac{1}{2}\left(\frac{B^2}{B_0}\right)\right]$$

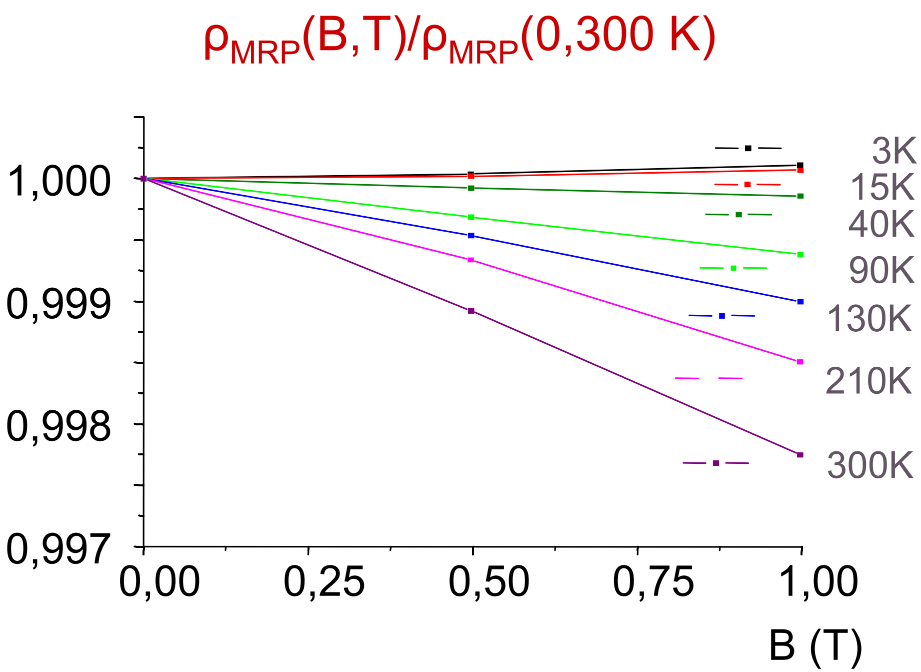

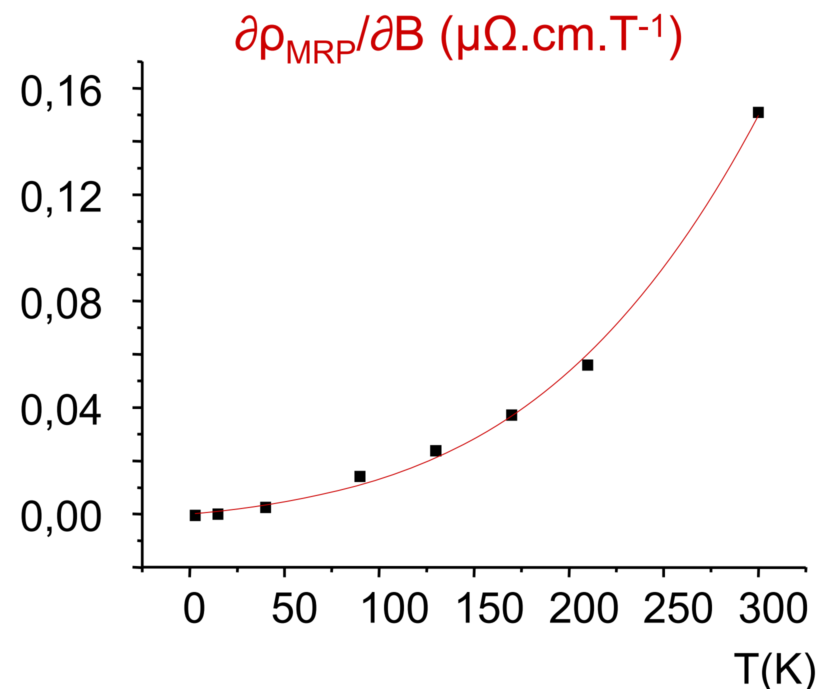

Temperature dependance

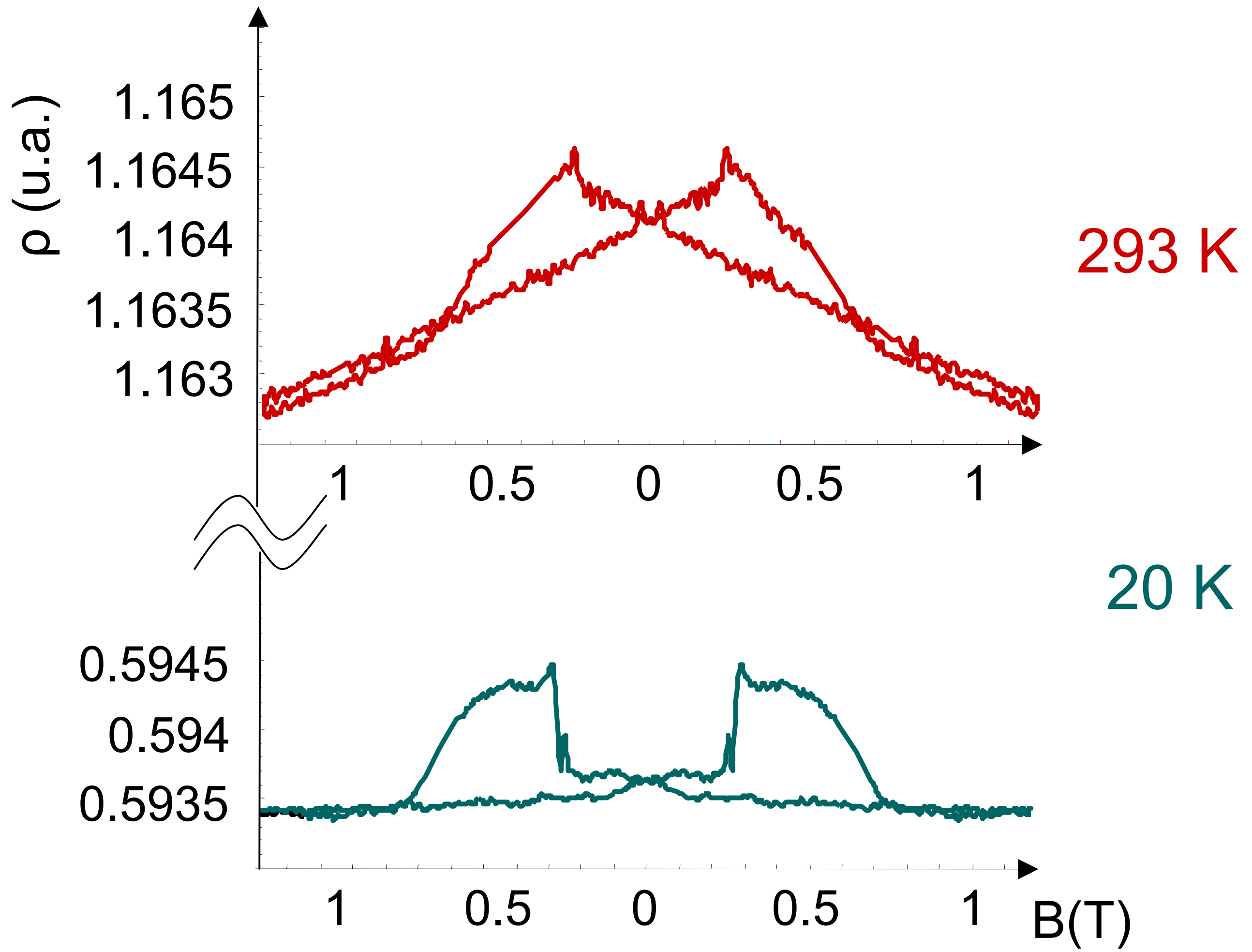

RESISTIVITY 40 microohms.cm

Bonus : spin-valve FePt/Pt/FePt

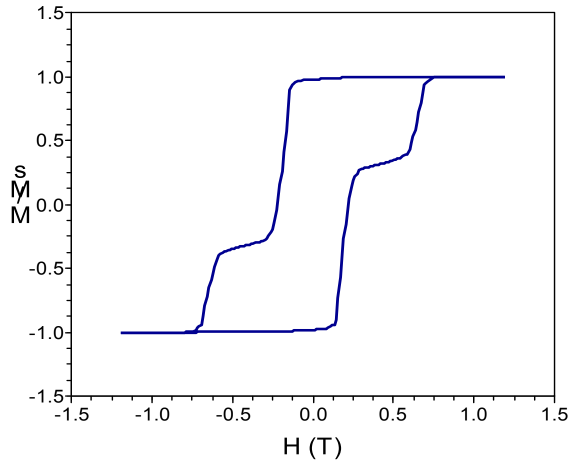

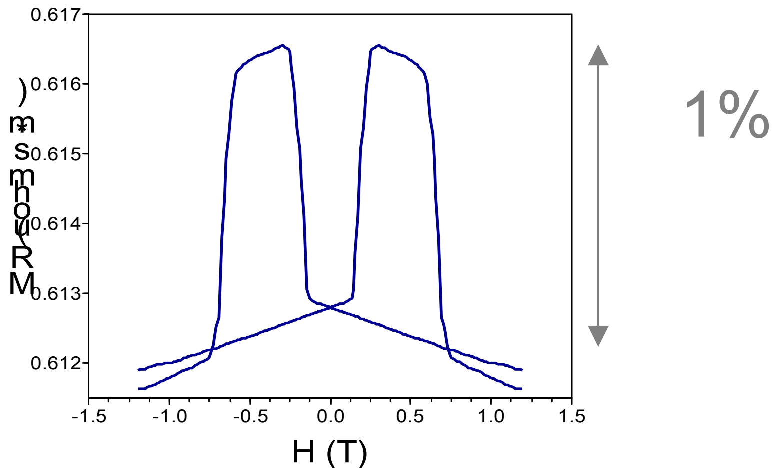

Interaction électrons magnons dans métaux 3d purs.

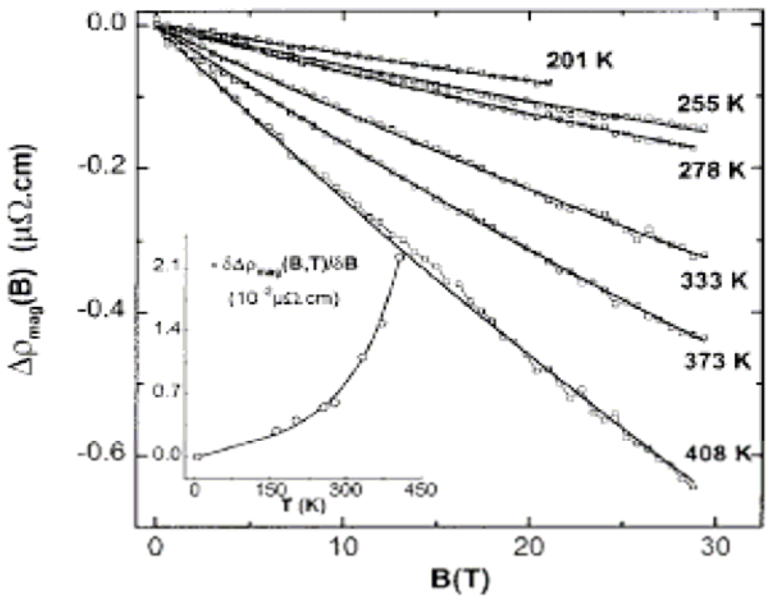

FIG. 4. Experimental high-field magnetic resistivity (open squares) and theoretical $\Delta\rho_{\mathrm{mag}}(B)$ curves (solid lines) deduced from Eq. (7) for $Fe_{80\,\mathrm{nm}}/MgO$ thin films with the band structure parameters listed in Table I and the magnon mass renormalization as only fitting parameters (see text). In the inset, the agreement between the experimental temperature dependence of the high-field MR slope (open circles) and the theoretical one (solid line).

$$\Delta\rho(T,B) \approx \rho(T,B) - \rho(T,0) \propto \frac{BT}{D(T)^2}\ln\left(\frac{\mu_B B}{kT}\right).$$

$$\left.\frac{\partial\Delta\rho_{\mathrm{mag}}(T,B)}{\partial B}\right|_{B \gg \mu_0 Ms} \propto T(1+2d_1T^2)(\ln T + cte),$$

Raquet et al.(Phys. Rev. B **66**, 024433 (2002))

Modèle interaction électrons-magnons

- Reprise du modèle de Raquet et al.

Idée: la bande « d » agit comme un piège avec une densité d'états forte dans laquelle les électrons « s » de conduction sont diffusés par l'intermédiaire des magnons

$$E(q) = Dq^2 + g\mu_B (B_{\text{int}\, erne} + B_A + B_D + \mu_0 M_S \sin^2 \theta_k)$$

;

Où :
- D est le terme de «raideur » de magnons,
- B est le champ extérieur appliqué, B_{int} est le champ interne

le dernier terme est la de désaimantation induite par les magnons

$$B_{\text{int}} = \mu_0 H + \mu_0 M_S = B + \mu_0 M_S$$

$$B_D = -\mu_0 M_S \qquad B_A = \mu_0 H_A$$

Modèle interaction électrons-magnons

$$B_t = B_{\text{int}\,erne} + B_A + B_D + \mu_0 M_S \sin^2 \theta_k$$

$$\Delta\rho \propto \frac{B_t}{D(T)^2} T \ln(\frac{\mu_B B_t}{kT})$$

Cas des métaux 3d purs (Raquet et al.):

•Faible anisotropie

•Fort champ appliqué

⇨ Bt=B

Notre cas:

•Forte anisotropie

•Faible champ appliqué

$$B_t = B + B_A + \mu_0 M_S$$

Modèle interaction électrons-magnons

$$\Delta\rho \propto \frac{B_t}{D(T)^2} T \ln\left(\frac{\mu_B B_t}{kT}\right)$$

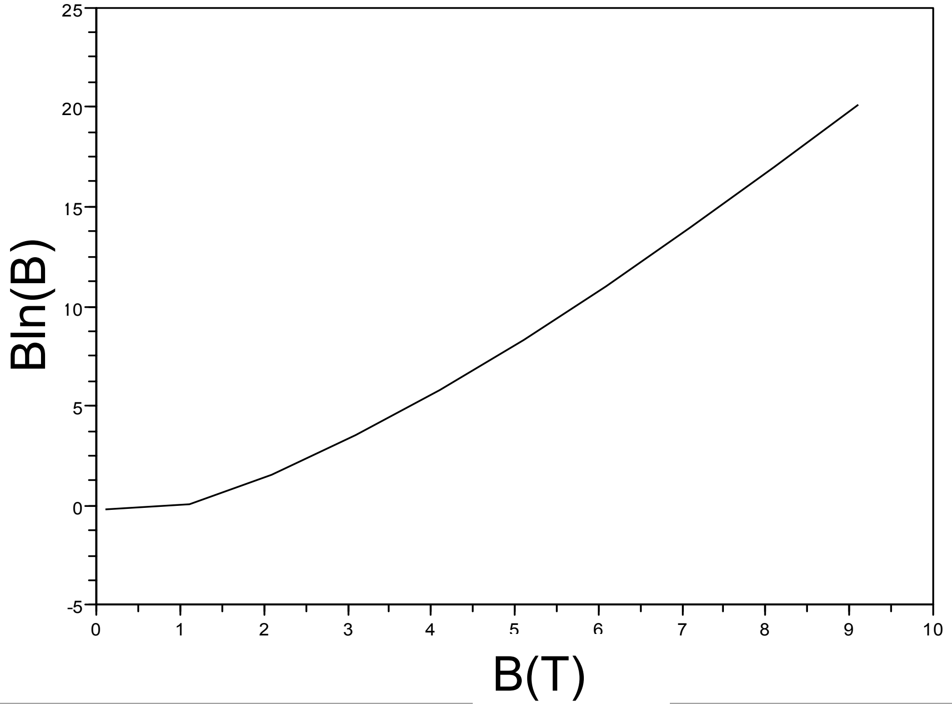

- Dans les deux cas:

Le terme $\left(\frac{\mu_B B_t}{kT}\right)$ Doit être >1 pour déterminer une variation linéaire de la MR(H)

Modèle interaction électrons-magnons rapporté à la mesure

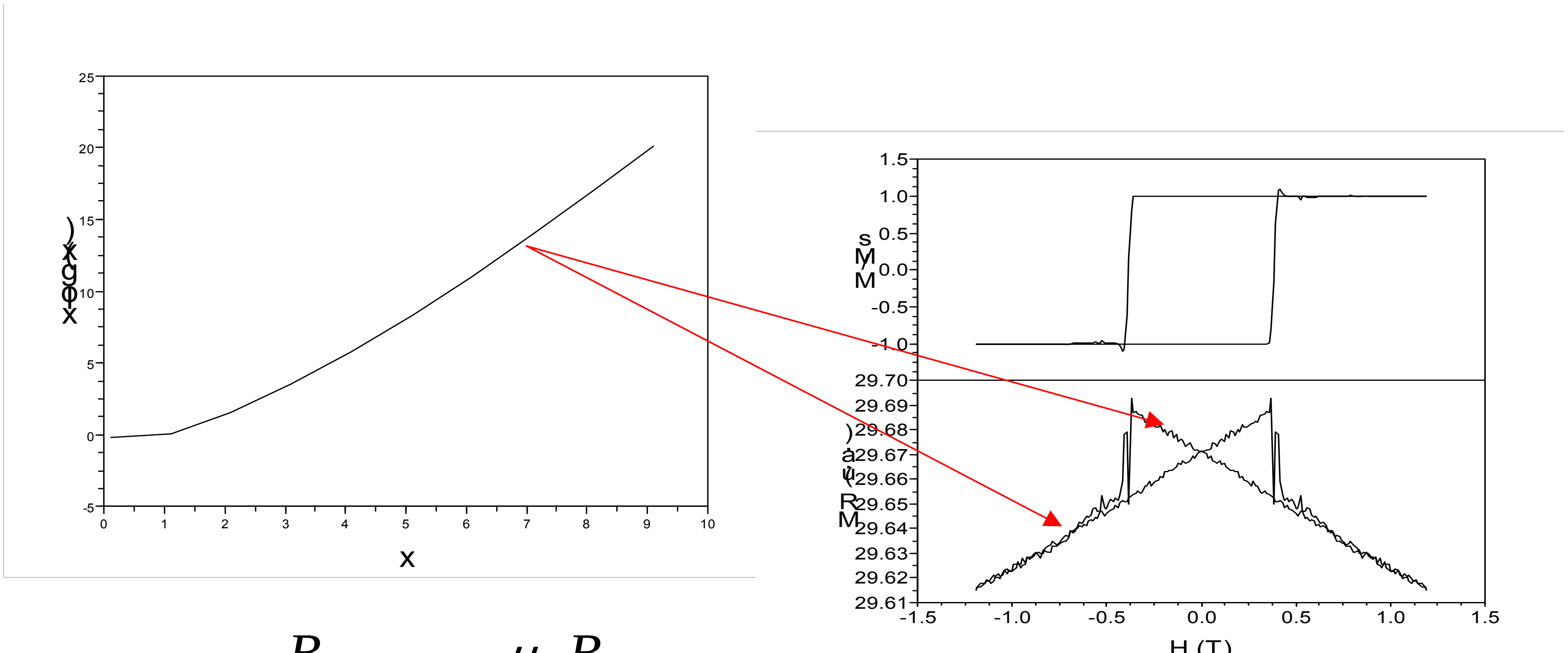

$$\Delta\rho \propto \frac{B_t}{D(T)^2} T \ln(\frac{\mu_B B_t}{kT})$$

Modèle interaction électrons-magnons

- Variation de la pente MR(H) fonction de T

Cas de Raquet:

Développement linéaire autour

des grands champs appliqués

$$\frac{\partial \Delta\rho(T)}{\partial B} \propto T(1+2d_1T^2)\left[\ln(T)+cte\right]$$

Notre cas:

Développement linéaire autour du zéro du champ applique mais Bt est toujours grand à cause de $B_{anisotropie}$

$$\frac{\partial \Delta\rho(T)}{\partial B} \propto \frac{1}{{D_0}^2} T(1+2d_1T^2)\left[\ln(T)-\ln\left(\frac{\mu_B B_t}{k}\right)-1-\frac{B}{B_t}+\tfrac{1}{2}\left(\frac{B^2}{B_t}\right)\right]$$

Détection renversement aimantation

- Difficile d’intégrer la contribution de MR de parois dans la détermination de l’aimantation
- Méthode limitée à des matériaux à forte anisotropie et épaisseur faible.

Conclusion

- Nous avons réussi à appliquer le modèle de Raquet *et al.* à des champs appliqués faibles dans le cas de matériaux à forte anisotropie
- Nous avons trouvé un nouveau moyen de de mesure d’aimantation dans des couches minces.